Linearized potential flow analysis of a 40 chamber, oscillating water column wave energy device

Bingham, Harry B.; Read, Robert

Publication date:
2015

Document Version
Peer reviewed version

Linearized potential flow analysis of a 40 chamber, oscillating water column wave energy device

Harry B. Bingham and Robert Read

Dept. of Mechanical Engineering, Technical University of Denmark

Email: hbb@mek.dtu.dk, rrea@mek.dtu.dk

This abstract presents an analysis of an attenuator-type Wave Energy Converter (WEC) with 40 Oscillating Water Column (OWC) chambers for the extraction of wave energy. Linearized potential flow calculations are made in the frequency-domain using WAMIT [8]. An equivalent linearized damping coefficient to represent the air turbine Power Take Off (PTO) system is found for each condition by iterating to find the consistent response-damping pair for a given frequency and incident wave amplitude. The absorbed power is estimated based on the pressure in each chamber and the PTO damping coefficient. The calculations are compared to model-scale measurements in a slack-moored condition, and generally good agreement is found. Work is in progress to move the solution to the time-domain and include a more sophisticated PTO model which includes nonlinear and air compressability effects in the turbine.

1 Theory

Evans [2], extended first-order, radiation-diffraction theory to include the response of one or more partially enclosed OWC chambers, together with the usual rigid-body motions. This theory was also discussed by Lee et al [3, 4] and it is implemented in WAMIT as Free-Surface Pressure (FSP) modes. The applied pressure on the water surface in each internal chamber is expressed in a modal decomposition of the form

$$p_0(x,y) = -\rho g \sum_{j=7}^{6+M_p} \xi_j \, n_j(x,y) \tag{1}$$

where n_j gives the spatial form of mode j and M_p is the total number of modes, with ρ the fluid density and g is the gravitational acceleration constant. Here we will only consider one piston-type mode for each OWC chamber, as this is the only mode that contributes to the flux through the turbine, thus M_p is the total number of chambers and $n_j = 1$ on chamber surface j. For the FSP modes, the boundary condition on the internal free surface becomes

$$\partial_z \phi - \frac{\omega^2}{g}\phi = -\frac{\mathrm{i}\omega}{\rho g} p_0 = \mathrm{i}\omega \sum_{j=7}^{6+M_p} \xi_j n_j, \quad \text{on } z = 0 \tag{2}$$

and ξ_j thus represents the pressure head response to a unit amplitude applied pressure on internal free-surface j, with ω the radian frequency of oscillation and ϕ the total velocity potential. This leads to an equation of motion of the same form as the rigid-body modes so that the complete system can be written in the standard non-dimensional form as

$$\sum_{k=1}^{6+M_p} \left[-\bar{\omega}^2 \left(\bar{M}_{jk} + \bar{A}_{jk} - \mathrm{i}\,\bar{B}_{jk} \right) - \frac{1}{\mathrm{i}\bar{\omega}} \bar{B}^0_{jk} + \bar{c}_{jk} \right] \bar{\xi}_k = \bar{X}_j, \qquad j = 1, 2, \ldots, 6 + M_p \tag{3}$$

with $M_{jk}, A_{jk}, B_{jk}, c_{jk}, X_j$ the inertia, added mass, damping, hydrostatic restoring and incident wave exciting force coefficients respectively. All quantities are made non-dimensional with respect to a length scale L, ρ, g, and the incident wave amplitude A; more details can be found in the WAMIT user manual [8]. The air turbine PTO damping coefficient matrix B^0_{jk} is diagonal, and only non-zero

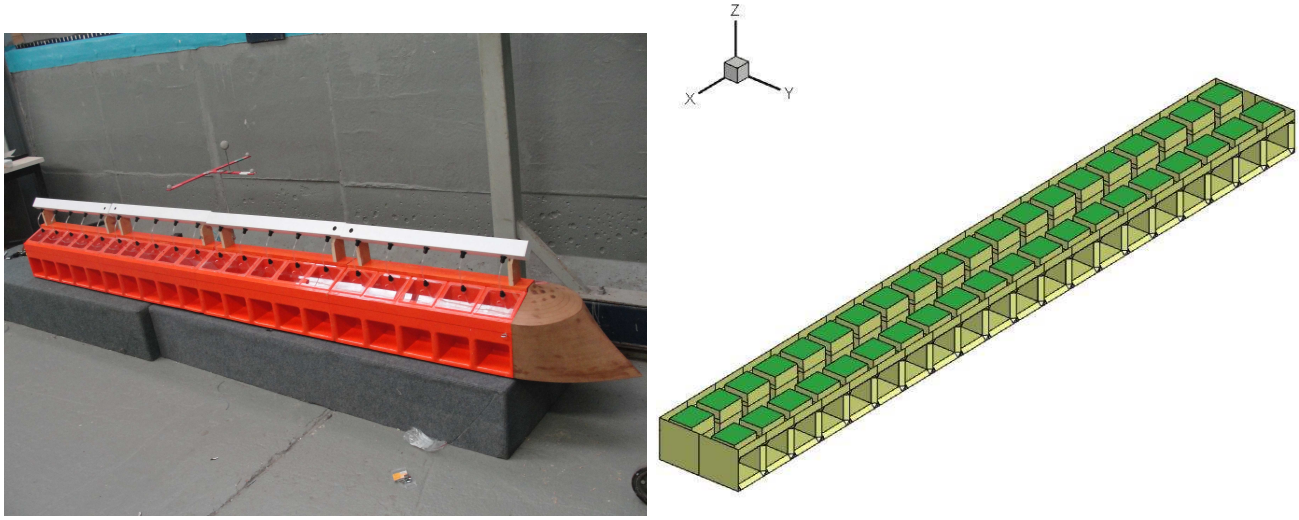

Figure 1: Left: Photo of the scale model ready for testing. A removable bow section is fitted in this picture, but results are presented here only without the bow. Right: The high-order geometry used for the WAMIT calculations. Bright green patches indicate the FSP surfaces.

for the FSP modes with $j > 6$, while all inertia terms associated with the FSP modes are zero. The new terms in the equation are given by

$$\bar{B}^0_{jj} = \frac{\rho\sqrt{gL}}{L^2} B_{j0}, \quad q_j = -\rho g\, B_{j0}\, \xi_j, \quad c_{jj} = -\frac{S_{j0}}{L^2} \tag{4}$$

where a linear relation has been assumed between the volume flux q_j through chamber j and the pressure in that chamber, and S_{j0} is the area of internal free-surface j. Since the structure itself must create the excess pressure in each chamber, there is hydrostatic coupling between the FSP modes and the heave, roll and pitch modes which must also be included in $\bar{c}_{jk}$. The total efficiency of the device can be written as a capture width ratio

$$\overline{W} = \frac{W}{W_{max}} = \sum_{j=7}^{6+M_p} \frac{\bar{B}_{j0}\, \bar{\xi}^*_j \bar{\xi}_j}{\bar{c}_g} \frac{L}{L_c} \tag{5}$$

where $\bar{c}_g = c_g/\sqrt{gL}$, with c_g the wave group velocity, and L_c the length-along-the-wave-crest chosen for normalization. More complete details of this formulation can be found in [1] along with a more complete presentation and discussion of the results shown here.

2 Results

Figure 1 shows a picture of the scale model and the patch boundaries of the high-order geometry used for the WAMIT calculations. This geometry was produced using the MultiSurf surface modeling software [7]. The FSP internal chamber surfaces are indicated by the bright green patches of the numerical model. The model was tested with and without the removable bow section shown in the picture, but here we consider only the data without the bow section. This design is a variant of the I-beam attenuator [6] which was inspired by the Kaimei concept developed in the late 1970s by Masuda and his colleagues in Japan [5]. The target installation area of the device is the Danish North Sea, so the full-scale chambers measure 6 by 5 by 7.5 m in the x, y and z directions respectively, which gives a resonant period of 5.9s. The total device length is $L = 150$m. The model is at scale 1:50 and was tested at the Hydraulic and Maritime Research Center (HMRC) at University College Cork, Ireland in 2013 [9, 10]. The air turbine PTO system was model led by an orifice in each chamber lid of 1.3%

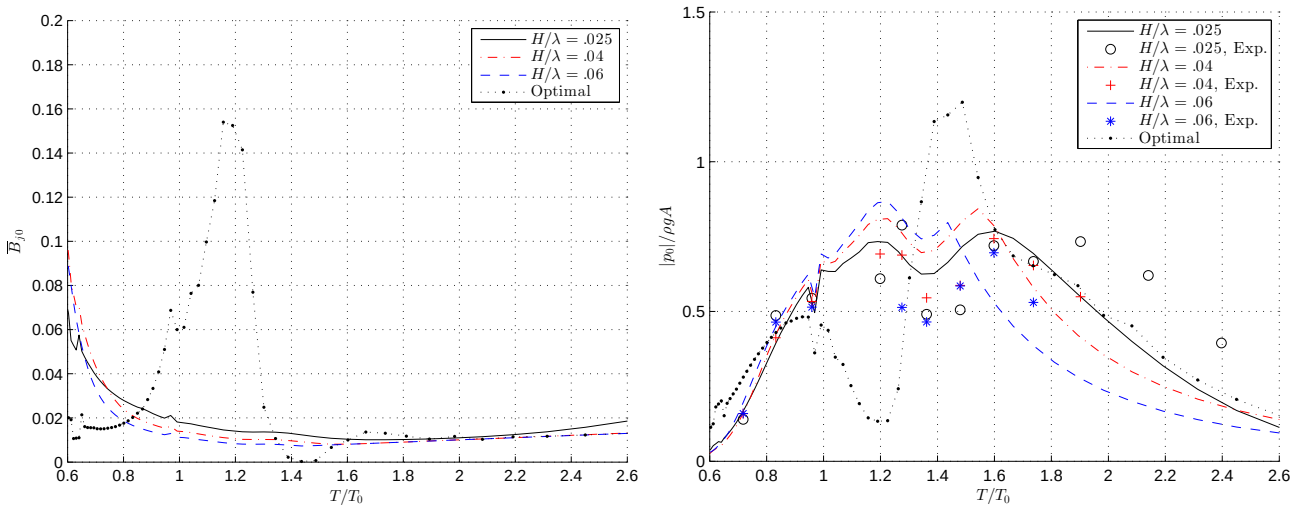

Figure 2: The equivalent linearized damping coefficient (left) and the pressure response (right) in the bow Chamber for the freely floating model.

of the chamber surface area. This is a good model of an impulse turbine, and produces a quadratic relation between the flux and the pressure in the chamber so that $q^2 = B_1|p|$. To find the equivalent linear damping coefficient B_{j0}, we equate the power loss over one cycle of the two relations which gives

$$B_{j0} = \sqrt{\frac{3\pi}{8\rho g|\xi_j|}}B_1. \tag{6}$$

The quadratic damping coefficient B_1 is a constant and has been accurately determined from a simple experiment. Since the equivalent linear damping coefficient is a function of the response amplitude however, we must iterate the solution of (3) and (6) for each incident wave frequency and amplitude. The initial guess is taken to be $\xi_j/A = 0.5$, and the solution generally converges to single precision accuracy in about 10 iterations or less.

The model has been tested at a series of mono-chromatic incident wave conditions corresponding to wave steepness values of $H/\lambda = 0.025, 0.04$ and 0.06, where $H = 2A$ is the wave height and λ is the wave length. The device is slack-moored and free to feather with the incoming waves so that they are always incident from ahead. Symmetry about the $y = 0$ plane is invoked, and the pressure is measured in all chambers along the starboard side of the vessel. The results for the equivalent linear damping coefficients and the pressure in chamber #1 at the bow of the model are shown in Figure 2. We have also computed a numerically optimized linear damping coefficient using the Matlab constrained optimization routine `fmincon`. In all cases, we have constrained the response to ensure that the chamber surface elevation does not exceed 2.5m which is the distance from the mean water level to the submerged chamber opening. The optimized values are also shown in the figure, along with the corresponding experimental measurements. Similar behavior is found for the other chambers. Figure 3 shows the predicted total absorbed power as a capture width ratio with respect to the length $L = 150$m, and also in MW for the full-scale device. The measured and computed chamber pressures and the total mean power absorption are in reasonably good agreement, though somewhat over-predicted near the resonant period and under-predicted in long waves.

We are now working on moving the numerical solution to the time-domain so that a more accurate model of the air turbine PTO system can be included in the calculations. Experimental results are also available in irregular wave conditions, and these will be compared with. Structural loading calculations are also in progress, in order to estimate the construction costs so that a cost of energy prediction can be made. One major advantage for OWC-type devices is the relative simplicity of the structure, with no moving parts in the water, which should allow for relatively inexpensive building materials

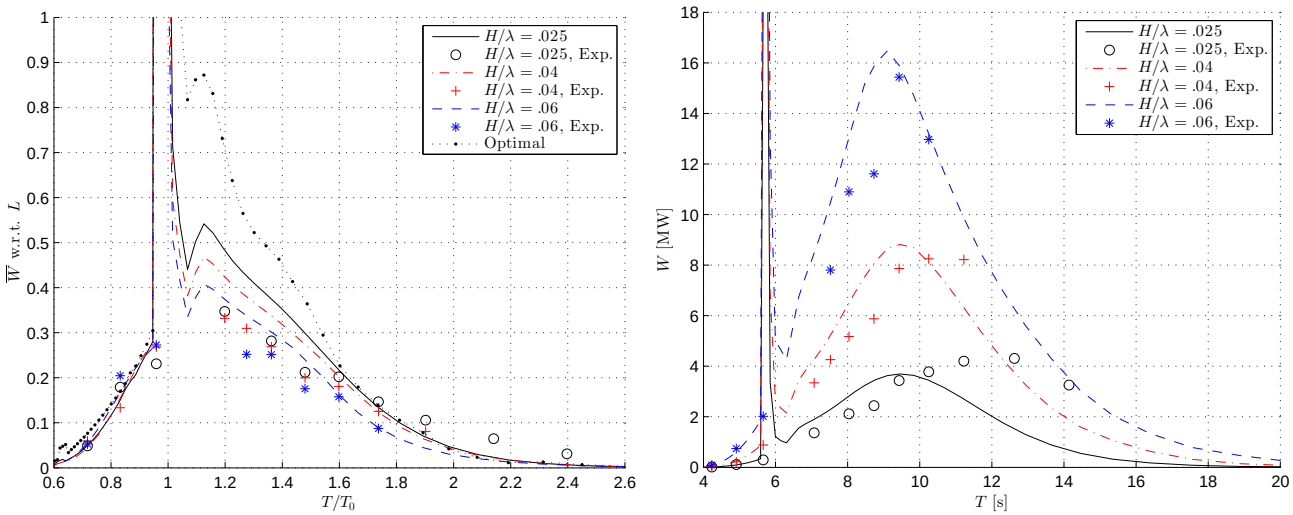

Figure 3: Left: The capture width ratio of the moored 40 chamber model with respect to $L = 150$m. Right: The corresponding full-scale power absorption in mega Watts.

and opportunities for mass production.

References

[1] H. B. Bingham, D. Ducasse, K. Nielsen, and R. Read. Hydrodynamic analysis of Oscillating Water Column, Wave Energy Devices. (Submitted), 2015.

[2] D. V. Evans. Wave-power absoption by systems of oscillating surface pressure distributions. *J. Fluid Mech.*, 114:481–499, 1982.

[3] C.-H. Lee, J. N. Newman, and F. G. Nielsen. Wave interactions with an oscillating water column. In 6^{th}*Intl. Offshore and Polar Engineering Conference*, Los Angeles, USA, 1996. Intl. Offshore and Polar Engineering Conference.

[4] C.-H. Lee and F. G. Nielsen. Analysis of oscillating water column device using a panel method. In 11^{th}*Intl. Wrkshp. Water Waves and Floating Bodies*, Hamburg, Germany, 1996. http://www.iwwwfb.org.

[5] Y. Masuda. Experimental full scale result of wave power machine Kaimei in 1978. In *Proc. 1st Inter. Symp. on Wave Energy Utilization*, Gothenburg, Sweden, 1979.

[6] G. W. Moody. The NEL oscillating water column: Recent developments. In *First Symposium on Wave Energy Utilization, Oct. 1979*, pages 283–296, Gothenburg, Sweden, 1980. Chalmers University of Tech.

[7] MultiSurf. AeroHydro - Relational 3D Modeling for Marine and Industrial Design, 2014. http://aerohydro.com.

[8] J. N. Newman and C.-H. Lee. Wamit; a radiation-diffraction panel program for wave-body interactions, 2014. http://www.wamit.com.

[9] K. Nielsen. Final report: KNSWING attenuator development phase I. Technical report, FP7-MARINET, Marine Renewables Infrastructure Network, 2013.

[10] F. Pors and M. Simonsen. A theoretical and experimental study of an Oscillating Water Column Attenuator. BS thesis, Tech. U. of Denmark, Lyngby, Denmark, 2013.